Journal of Advanced Research 65 (2024) 283–295

Contents lists available at ScienceDirect

Journal of Advanced Research

journal homepage: www.elsevier.com/locate/jare

Slow gut transit increases the risk of Alzheimer's disease: An integrated study of the bi-national cohort in South Korea and Japan and Alzheimer's disease model mice

Jiseung Kang [a,b,c,1], Myeongcheol Lee [d,e,1], Mincheol Park [a], Jibeom Lee [a], Sunjae Lee [f], Jaeyu Park [d,e], Ai Koyanagi [g], Lee Smith [h], Christa J. Nehs [b,c], Dong Keon Yon [d,e,i,*], Tae Kim [a,*]

[a] Department of Biomedical Science and Engineering, Gwangju Institute of Science and Technology, Gwangju, Republic of Korea
[b] Department of Anesthesia, Critical Care and Pain Medicine, Massachusetts General Hospital, Boston, MA, United States
[c] Division of Sleep Medicine, Harvard Medical School, Boston, MA, United States
[d] Center for Digital Health, Medical Science Research Institute, Kyung Hee University Medical Center, Kyung Hee University College of Medicine, Seoul, Republic of Korea
[e] Department of Regulatory Science, Kyung Hee University, Seoul, Republic of Korea
[f] School of Life Sciences, Gwangju Institute of Science and Technology, Gwangju, Republic of Korea
[g] Research and Development Unit, Parc Sanitari Sant Joan de Deu, Barcelona, Spain
[h] Centre for Health, Performance and Wellbeing, Anglia Ruskin University, Cambridge, UK
[i] Department of Pediatrics, Kyung Hee University Medical Center, Kyung Hee University College of Medicine, Seoul, Republic of Korea

HIGHLIGHTS

- Constipation was associated with an increased risk of Alzheimer's disease (AD) in the South Korean cohort (discovery cohort, HR, 2.04; 95% CI, 2.01–2.07) and the Japan cohort (validation cohort, HR, 2.82; 95% CI, 2.61–3.05).
- Loperamide-treated AD mouse model showed increased amyloid-beta and microglia in the brain with slow gut transit.
- Loperamide-treated AD mouse model had increased transcription of genes related to norepinephrine secretion and immune responses and decreased transcription of defense against bacteria in colonic tissue.

GRAPHICAL ABSTRACT

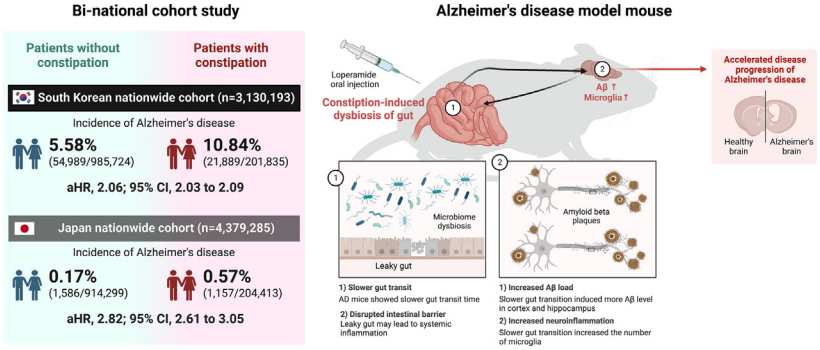

ARTICLE INFO

Article history:
Received 17 September 2023
Revised 20 November 2023
Accepted 12 December 2023
Available online 13 December 2023

Keywords:
Alzheimer's disease
Cohort

ABSTRACT

Introduction: Although the association between Alzheimer's disease (AD) and constipation is controversial, its causality and underlying mechanisms remain unknown.
Objectives: To investigate the potential association between slow gut transit and AD using epidemiological data and a murine model.
Methods: We conducted a bi-national cohort study in South Korea (discovery cohort, N=3,130,193) and Japan (validation cohort, N=4,379,285) during the pre-observation period to determine the previous diagnostic history (2009–2010) and the follow-up period (2011–2021). To evaluate the causality, we induced slow gut transit using loperamide in 5xFAD transgenic mice. Changes in amyloid-beta (Aβ) and other

* Corresponding authors at: Center for Digital Health, Medical Science Research Institute, Kyung Hee University Medical Center, Kyung Hee University College of Medicine, Seoul, Republic of Korea (D. K. Yon); Department of Biomedical Science and Engineering, Gwangju Institute of Science and Technology, Gwangju, Republic of Korea (T. Kim).
E-mail addresses: yonkkang@gmail.com (D.K. Yon), tae-kim@gist.ac.kr (T. Kim).
[1] These authors contributed equally to this work.

https://doi.org/10.1016/j.jare.2023.12.010

Constipation
Epidemiological data
Mouse model
Gut-brain axis

markers were examined using ELISA, qRT-PCR, RNA-seq, and behavioral tests.
Results: Constipation was associated with an increased risk of AD in the discovery cohort (hazard ratio, 2.04; 95% confidence interval [CI], 2.01–2.07) and the validation cohort (hazard ratio; 2.82; 95% CI, 2.61–3.05). We found that loperamide induced slower gut transit in 5xFAD mice, increased Aβ and microglia levels in the brain, increased transcription of genes related to norepinephrine secretion and immune responses, and decreased the transcription of defense against bacteria in the colonic tissue.
Conclusion: Impaired gut transit may contribute to AD pathogenesis via the gut-brain axis, thus suggesting a cyclical relationship between intestinal barrier disruption and Aβ accumulation in the brain. We propose that gut transit or motility may be a modifiable lifestyle factor in the prevention of AD, and further clinical investigations are warranted.

Introduction

Constipation is a common gastrointestinal condition in elderly individuals [1] with a global pooled prevalence of 10 to 15 % in community-dwelling elderly people [2]. It is characterized by hard or dry stools, incomplete bowel evacuation, and a reduced frequency of defecation [2,3]. The incidence of constipation increases with age [2]; the overall prevalence is 8.2 %, while it is 18.1–35.8 % in individuals over 60 years of age [4]. Constipation is associated with various neurological and neurodegenerative diseases, including Parkinson's disease (PD) and Lewy-body dementia [5,6], and it is a common symptom in over half of the patients with PD [6]. Similarly, patients with dementia and Alzheimer's disease (AD) frequently have constipation. However, constipation has rarely been studied in AD, although it is identified in approximately 17.2 % of patients with AD [7]. Despite these indications, previous investigations on the relationship between AD and constipation have used limited sample sizes with limited and inconclusive results [6–8]. Our study aimed to bridge this research gap by using large-scale bi-national cohorts from South Korea and Japan to comprehensively investigate this association.

Gastrointestinal dysfunctions, including diarrhea and constipation, are frequently associated with peripheral nerve damage and autonomic neuropathy [9,10]. In patients with dementia, constipation may also be a manifestation of autonomic nerve dysfunction [11–13]. Therefore, constipation can be considered a neurological symptom, with the sympathetic and parasympathetic nervous systems playing important roles in its development and progression [14]. The etiologies of constipation and AD remain unknown; however, according to a comparative epidemiological investigation, they share common risk factors such as sex, age, economic status, and dietary habits [15]. Furthermore, several reports have suggested that dysfunctions in the gut-brain axis and alternations in the gut microbiota can contribute to the occurrence of both diseases [16–19]. The gut-brain axis refers to the bidirectional communication between the gut and the central nervous system (CNS). This axis is believed to play a crucial role in the relationship between CNS disorders and the onset and progression of constipation [20]. Constipation or slow gut transit can alter the gut microbiome, which can affect the gut-brain axis in turn, contribute to the development of constipation through alterations in the gut transit time [21]. Furthermore, constipation can result in gut dysbiosis, thus further exacerbating imbalances in the gut-brain axis and potentially contributing to other neurological conditions [22–24]. Although studies have investigated the changes in the gut microbiome in patients with AD or AD mouse models, evidence regarding whether functional abnormalities in the gut can provoke the pathology of AD in the brain remains lacking [24–28].

The limited sample sizes and observational designs of previous studies have resulted in an incomplete picture of the relationship between AD and constipation [4,6–8]. Our study fills this gap by utilizing large-scale bi-national cohorts from South Korea and Japan to investigate this association. In addition, we investigated these associations and underlying mechanisms in an animal model as a proof-of-concept test. The large-scale bi-national cohorts provide insights into the epidemiology of the association between AD and constipation, while the AD mouse model is a controlled investigation of the pathological mechanisms at play. A previous study found that AD model mice showed parameters of constipation in the stools as well as in the histological structure of the colon [29]. However, they only used stool morphology as a marker of constipation and did not evaluate gut transit. Furthermore, the study was an observational one, and therefore, the causal relationship between AD and constipation remains unknown. We hypothesized that constipation is linked to an increased risk of AD and its pathology in the brain via the gut-brain axis. Consequently, we aimed to examine the potential association between constipation and AD using a bi-national cohort (Japan and South Korea) and a murine model of AD.

Methods

Epidemiological model

We used bi-national, general, population-based, large-scale cohorts from South Korea (discovery cohort, N = 3,130,193) and Japan (validation cohort, N = 4,379,285) to explore the relationship between AD and constipation. This study was approved by the Institutional Review Boards of the Kyung Hee University (approval no. KHUH 2022-06-042). The requirement for informed consent was waived because the study used anonymized data.

In both cohorts, the 'exposure' was constipation, the 'primary outcome' was incident AD, and the 'individual index date' was the date of the first constipation diagnosis or the matched date within the control cohort to mitigate any potential bias related to immortality. The pre-observation period to determine the diagnostic history was 2009–2010, and the follow-up period was 2011–2021. The follow-up ended on December 31, 2021, or with the death of the participant, whichever was earlier. Detailed methodologies are described in the Supplementary Materials.

Animals

Transgenic hemizygous 5XFAD mice that overexpressed Swedish, Florida, and London mutants of human APP and M146L and L286V mutants of human PS1 under the control of the Thy1 promoter were used in the experiments (Jackson Laboratory, Bar Harbor, ME, USA). These mice demonstrated an extracellular Amyloid-beta (Aβ) accumulation and impaired memory functions at 6 months of age [30]. The animal procedures were approved by the ethics committee of a Gwangju Institute of Science and Technology (approval no. GIST-2020–031) following the Institutional

Animal Care and Use Committee. The mice received a standard chow diet (RodFeed, DBL, Eumseong, Republic of Korea) based on the NIH-41 Open Formula ad libitum under a 12-h light/dark cycle (lights on 7 pm) with a constant temperature and humidity of 20 ± 2 ℃ and 55 ± 5%.

Seven-month-old 5XFAD transgenic (n = 6, male) and wild-type (n = 5, male) mice were assigned to TG and WT groups, respectively. We established an AD mouse model with loperamide-induced constipation by modifying a method reported previously (Table S1). To examine the effects of loperamide-induced constipation on AD, five-month-old 5XFAD transgenic mice and wild-type mice were randomly assigned to four groups: i) TG-loperamide (Lop) group mice (n = 4) were administered oral loperamide each week dissolved in saline at a dose of 5 mg/kg body weight for 4 weeks; ii) TG-control (Con) group mice (n = 5) were administered oral saline for 4 weeks; iii) WT-lop group mice (n = 4) were orally injected each week with loperamide doses of 5 mg/kg body weight for 4 weeks, and iv) WT-con group mice (n = 3) were orally administrated saline only for 4 weeks.

Behavioral test

The open field test (OFT) and novel place recognition (NPR) tests were conducted consecutively over 3 days during the dark period (between 7 pm and 11 pm) in a separate sound-attenuated room. On the first day, the OFT was used to assess the locomotor activity and anxiety levels of the mice in a novel testing arena (40 × 40 × 40 cm square testing arena under dim red light of approximately 50 lx). The mice were gently placed in the center of the empty test chamber and allowed to move freely for 10 min.

The NPR test, which examines visuospatial memory, was conducted over the next 2 days. The second day (acquisition trial for the NPR test) involved the placement of two identical objects in the same position relative to the visual cue on the test box wall and the mice were allowed to explore for 10 min. On the third day (test trial of the NPR test), an object was moved to a new location, and the mice were allowed to explore the familiar and new locations for 10 min. In order to calculate the discrimination index, which reflects the relative preference for the new location, the following formula was used: discrimination index = (time spent in novel location - time spent in familiar location)/(time spent in novel location + time spent in familiar location) [31]. A video tracking system, Smart 3 (Panlab, Harvard Apparatus, Barcelona, Spain), was used to record and analyze the data.

Measurement of gut transit

Six groups, including male 7-month-old TG and WT groups and 6-month-old TG-Lop, TG-Con, WT-Lop, and WT-Con groups, were fasted for 12–16 h. Then, 100 μL of 5 mg/mL 70-kDa FITC dextran (46945, Sigma Aldrich, Burlington, MA, USA) in saline was administered orally in a single dose. In each mouse, the entire gastrointestinal tract was harvested after 30 min and divided into the following segments: stomach (#1), 10 equal segments of the small intestine (#2–11), cecum (#12), and three equal of the colon (#13–15). After fractionation of the gastrointestinal tract, the luminal contents were collected in 1 mL of phosphate-buffered saline (PBS). The stomach and cecum were chopped in 1 mL PBS. The luminal contents were centrifuged for 10 min at 12,000 rpm, and the fluorescence intensity of the resulting supernatant was measured at 485 nm (absorption) and 528 nm (emission). As a measure of gastrointestinal motility, the geometric center (GC) of the distribution was calculated using the following formula: GC = Σ(% of total fluorescent signal per segment × segment number)/100.

Tissue collection

The mice were anesthetized with isoflurane, and the abdominal aorta was clamped to ensure that the brain was completely exsanguinated. Next, they were transcardially perfused with 1X PBS. The brain is divided into two hemispheres. The right hemispheres were dissected to separate the frontal cortex, hippocampus, and brainstem and stored at −80 °C until analysis. The colon was harvested and stored in RNAlater™ Stabilization Solution (AM7020, Thermo Fisher Scientific, Waltham, MA, USA) at −80 ℃ until analysis.

Enzyme-linked immunosorbent assay (ELISA)

The cortex, hippocampus, and brainstem were individually homogenized using a disposable polypropylene pellet pestle in 800 mL of a buffer solution containing 5 mM EDTA, 20 mM Tris-HCl (pH 7.8), and a protease inhibitor cocktail (P3100, GenDEPOT, Katy, TX, USA). The Micro BCA™ Protein Assay kit (23225, Thermo Fisher Scientific, Waltham, MA, USA) was used to determine the total protein content of the homogenates. Using a Beckman TLA 100.3 centrifuge rotor (Beckman Coulter, Inc., Fullerton, CA, USA), the homogenates were centrifuged for 20 min at 4 °C and 430,000 rcf. A pestle was used to homogenize the remaining insoluble pellets in 800 mL of buffer solution containing 5 mM guanidine hydrochloride (GHCl) and 50 mM Tris-HCl (pH 8.0), and the solution was agitated for 4 h. A Beckman TLA 100.3 centrifuge rotor was used to centrifuge the mixture at 4 °C and 430,000 rcf for 20 min, and the supernatant was collected as insoluble Aβ42. ELISA was performed to quantify the soluble and insoluble Aβ42 as per the manufacturer's protocol (KHB3441, Thermo Fisher Scientific, Waltham, MA, USA).

RNA preparation and quantitative reverse transcriptase PCR (qRT-PCR)

RNA was extracted from the colon samples utilizing the TRI reagent (TR118, Molecular Research Center, Ohio, USA) according to the manufacturer's protocol. The extracted RNA (2.5 μg) was reverse transcribed into cDNA through the use of oligo(dT)18 primers (RT200, TOPscript™ RT DryMIX [dT18 plus], Enzynomics, Daejeon, Korea) following a 60-minute incubation window at 50 °C and a subsequent 5-minute inactivation step at 95 °C. Gene expression was determined through qRT-PCR, using 1 μL of cDNA as a template, and amplified with TOPreal qPCR 2x PreMIX (RT5015, Enzynomics, Daejeon, Korea). The relevant primers were synthesized by Macrogen (Seoul, Korea) and are listed in Table S2. The expression data were processed using StepOne Plus™ software (Applied Biosystems, Waltham, MA, USA) through 40 cycles, with each cycle consisting of 15 s of annealing at 60 °C and 30 s of elongation at 72 °C. The fold change in gene expression was calculated using the $2^{-\Delta\Delta Ct}$ method to determine the differentially expressed genes in each group.

Whole transcriptome analysis

Colon RNA samples were sequenced using the TruSeq Stranded Total RNA Sample Preparation Kit with Ribo-Zero H/M/R (Illumina, San Diego, CA, USA). On a NovaSeq 6000 system (Illumina, San Diego, CA, USA), 150 bp paired-end sequencing was conducted with 50 million reads per sample. The pipelines used to analyze the RNA-seq data are shown in Fig. S1. Quality checks and adaptor trimming were performed using FASTQC v0.11.9 and Trimmomatic v0.38. The fastq data file was aligned with the mouse database (GRCm38) using HISAT2. HISAT2 provides two separate files—the mapped bam file and the unmapped FASTQ files.

Quantification of the transcript amount of the mapped BAM -files was conducted using FeatureCounts. The list of differentially expressed genes (DEGs) was normalized and extracted using the DESeq2 packages in R. A volcano plot was created to compare the DEG analysis results with a p-value cutoff of 0.05 and an absolute value of the log2 fold-change of 2. For pathway enrichment analysis, Gene Set Enrichment Analysis (GSEA) v4.3.2. was used with the Gene Ontology (GO) biological process database, and the input data included significant values from the DESeq2 results with a p-value cutoff of 0.05 and |log2FC| cutoff of 1. KEGG 2021 Human Pathway Analysis and Elsevier Pathway Collection in Enrichr (version. 2023.02) were used in this study.

To assign taxonomic labels to the metagenomic sequences, unmapped fastq files were processed using Kraken2 v2.1.1 at usegalaxy.org. A vegan package v2.6–4 in R was used to analyze and visualize the data as boxplots and Non-metric multi-dimensional scaling (NMDS) plots.

Immunohistochemistry

The left hemisphere of the murine brain was fixed in a 4% paraformaldehyde solution at pH 7.2 in PBS and placed in a 30% sucrose solution in PBS at 4 °C until it had sunk. A cryotome (Leica Biosystems, Buffalo Grove, IL, USA) was used to section the brain into 40-μm thick coronal sections. Subsequently, three rounds of washing with PBS containing 1% Triton X-100 (PBST) were performed for 10 min with shaking at 100 rpm at room temperature. Following this, the sections were blocked in a solution containing 3% normal donkey serum (D9633; Sigma Aldrich, St. Louis, MO, USA) in 0.5% PBST for 2 h at room temperature. To visualize the microglia, the primary antibody rabbit anti-Iba1 (1:1000, 019–19741, Wako, Japan) was used in combination with the secondary donkey anti-rabbit IgG antibody (1:500, A31572, Invitrogen, Waltham, MA). Similarly, to stain the astrocytes, a primary rabbit anti-GFAP antibody (1:1000, 019–19741, Wako, Japan) was used in combination with a secondary donkey anti-rabbit IgG antibody (1:500, A31572, Invitrogen, Waltham, MA). Aβ plaques were stained using 1 mM Thioflavin S (T1892, Sigma Aldrich, St Louis, MO, USA). As a next step, the section was mounted on slide glass coated with saline (5116-20F, Muto Pure Chemicals, Tokyo, Japan).

Quantification of Aβ plaques, microglia, and astrocyte

Histological images of four serial coronal sections from the cortex (at AP + 1.3 mm from the bregma), hippocampus (at AP-1.6 mm from the bregma), and brainstem (at AP-6.3 mm from the bregma) were collected with a research slide scanner (VS200, Olympus, Tokyo, Japan). To quantify the Aβ plaques, microglia, and astrocytes, the ImageJ software and an unbiased stereological dissector method were utilized. Representative images from the primary motor cortex, primary sensory cortex, and nucleus tractus solitarius were obtained using confocal microscopy (FV3000RS, Olympus, Tokyo, Japan) with a 40x objective lens and 38-μm thick sections and a 10-μm optical dissector height with 1 μm between images.

Quantification and statistical analysis

All data were analyzed with usegalaxy.org, R Studio (R Studio, Boston, MA, USA), and GraphPad Prism v9 (GraphPad Software, Inc., La Jolla, CA, USA) and presented as the means ± standard error of the mean (SEM).

Results

Association between AD and constipation in the discovery cohort (South Korea) and validation cohort (Japan)

A comprehensive analysis was performed on 7,509,478 participants, including 3,130,193 participants in the discovery cohort (mean follow-up: 6.48 years) and 4,379,285 participants in the validation cohort (mean follow-up: 6.10 years) (Fig. S2-4). The demographic and baseline characteristics of the cohorts after matching are shown in Table S3.

Overall, patients with constipation had 2.06 times (adjusted hazard ratio[aHR], 2.06; 95% confidence interval [CI], 2.03–2.09) greater likelihood in the discovery cohort and 2.82 times (aHR, 2.82; 95% CI, 2.61–3.05) greater likelihood in the validation cohort of developing AD after adjustments for confounders (Table 1). Furthermore, we found that patients with constipation for 1–3 years were more susceptible to AD (discovery cohort: aHR, 2.37; 95% CI, 2.29–2.45; and validation cohort: aHR, 3.14; 95% CI, 2.75–3.59) and this risk remained and persisted over 3 years (discovery cohort: aHR, 2.01; 95% CI, 1.98–2.05; validation cohort: aHR, 2.82; 95% CI, 2.57–3.10). Subgroup analyses according to sex, age, and disease duration demonstrated consistent results regarding the association between incident AD and constipation (Table S4).

Slower gastrointestinal transit in AD mice

We measured the lengths of the small intestine and colon to determine the general condition of the gastrointestinal system in 5xFAD transgenic mice. The lengths of the small intestine and colon were not significantly different between the TG and WT groups (Fig. 1A, B). However, the TG group demonstrated a lower stool weight normalized to body weight (Fig. S5A), a morphologically disorganized gut, and more adipose tissue surrounding the intestine compared with the WT group (Fig. S5B, C).

To investigate whether the pathological phenotypes of AD affect gut motility in TG mice, we measured the gut transit time by analyzing the distribution profiles of 70 kDa FITC-dextran using relative fluorescence units (RFU) and the distribution of FITC-dextran. The results revealed that the overall gut transit was slower in the TG group, with delayed peaks observed in the FITC-distribution plot (Fig. 1C, D). The cumulative distribution of FITC-dextran in the TG group was also delayed compared to that in the WT group (Fig. 1E). Additionally, the TG group showed lower geometric center (GC) values, thus indicating a slower gut transit time than that in the WT group (Fig. 1F).

Establishing a 'slow gut model' using loperamide

To induce slow gut transit in 5XFAD transgenic mice, we created a slow gut transit model in which loperamide, an antidiarrheal medication that slows gut motility, was administered. Loperamide did not affect the length of the small intestine (Fig. 2A) or the colon (Fig. 2B). However, a delayed gut transit time was observed in the form of delayed peaks of RFU and the distribution of FITC-dextran in the loperamide-treated TG group compared to the TG-Con group (Fig. 2C, D). The cumulative distribution of FITC-dextran in the TG-Lop group was also significantly delayed compared with that in the control group (Fig. 2E), and the TG-Lop group demonstrated a decreased geometric center (Fig. 2F). In the WT group, loperamide did not alter the length of the gastrointestinal tract or the gut transit time (Fig. S6A-F).

Table 1
Hazard ratios for the risk of incident AD following constipation diagnosis of subjects in the discovery and validation cohort after propensity score-matching.

	HR (95% CI)					
	Discovery cohort			Validation cohort		
Parameter (constipation)	Crude	Minimally adjusted[1]	Fully adjusted[2]	Crude	Minimally adjusted[1]	Fully adjusted[3]
Overall						
None	1.0 (reference)	1.0 (reference)	1.0 (reference)	1.0 (reference)	1.0 (reference)	1.0 (reference)
Patients with constipation	**2.04**	**2.07**	**2.06**	**3.29**	**3.19**	**2.82**
	(2.01 to 2.07)	**(2.03 to 2.10)**	**(2.03 to 2.09)**	**(3.05 to 3.55)**	**(2.96 to 3.44)**	**(2.61 to 3.05)**
Constipation duration, years						
None	1.0 (reference)	1.0 (reference)	1.0 (reference)	1.0 (reference)	1.0 (reference)	1.0 (reference)
<1	**1.59**	**1.90**	**1.97**	**3.09**	**2.94**	**2.55**
	(1.53 to 1.65)	**(1.83 to 1.97)**	**(1.90 to 2.04)**	**(2.70 to 3.54)**	**(2.57 to 3.37)**	**(2.22 to 2.92)**
1–3	**2.26**	**2.35**	**2.37**	**3.74**	**3.52**	**3.14**
	(2.18 to 2.34)	**(2.27 to 2.43)**	**(2.29 to 2.45)**	**(3.28 to 4.28)**	**(3.08 to 4.02)**	**(2.75 to 3.59)**
≥3	**2.11**	**2.04**	**2.01**	**3.22**	**3.18**	**2.82**
	(2.07 to 2.15)	**(2.01 to 2.08)**	**(1.98 to 2.05)**	**(2.94 to 3.53)**	**(2.90 to 3.49)**	**(2.57 to 3.10)**
Stratication analysis						
Male						
None	1.0 (reference)	1.0 (reference)	1.0 (reference)	1.0 (reference)	1.0 (reference)	1.0 (reference)
Patients with constipation	**2.42**	**2.37**	**2.32**	**3.65**	**3.59**	**3.18**
	(2.36 to 2.48)	**(2.31 to 2.43)**	**(2.27 to 2.38)**	**(3.30 to 4.04)**	**(3.24 to 3.97)**	**(2.87 to 3.53)**
Female						
None	1.0 (reference)	1.0 (reference)	1.0 (reference)	1.0 (reference)	1.0 (reference)	1.0 (reference)
Patients with constipation	**1.82**	**1.89**	**1.90**	**2.87**	**2.73**	**2.41**
	(1.79 to 1.86)	**(1.86 to 1.93)**	**(1.86 to 1.94)**	**(2.56 to 3.22)**	**(2.43 to 3.07)**	**(2.14 to 2.71)**
50–70 years old						
None	1.0 (reference)	1.0 (reference)	1.0 (reference)	1.0 (reference)	1.0 (reference)	1.0 (reference)
Patients with constipation	**2.66**	**2.66**	**2.68**	**3.24**	**3.23**	**2.87**
	(2.58 to 2.74)	**(2.58 to 2.74)**	**(2.60 to 2.76)**	**(2.94 to 3.57)**	**(2.94 to 3.56)**	**(2.61 to 3.17)**
Over 70 years old						
None	1.0 (reference)	1.0 (reference)	1.0 (reference)	1.0 (reference)	1.0 (reference)	1.0 (reference)
Patients with constipation	**1.86**	**1.88**	**1.87**	**3.11**	**3.11**	**2.74**
	(1.82 to 1.89)	**(1.85 to 1.92)**	**(1.84 to 1.91)**	**(2.75 to 3.52)**	**(2.74 to 3.51)**	**(2.41 to 3.11)**

AD, Alzheimer disease; CI, Confidence interval; HR, Hazard ratio.
[1] Minimally adjusted: adjustment for age (50–70 and over 70 years) and sex.
[2] Additionally adjusted: adjusted for age, sex, region of residence (urban and rural), Charlson comorbidity index, body mass index, systolic blood pressure, diastolic blood pressure, fasting blood glucose, serum total cholesterol, household income, smoking status, alcoholic drinks frequency, sufficient aerobic physical activity. Numbers in boldface correspond to significant differences ($P < 0.05$).

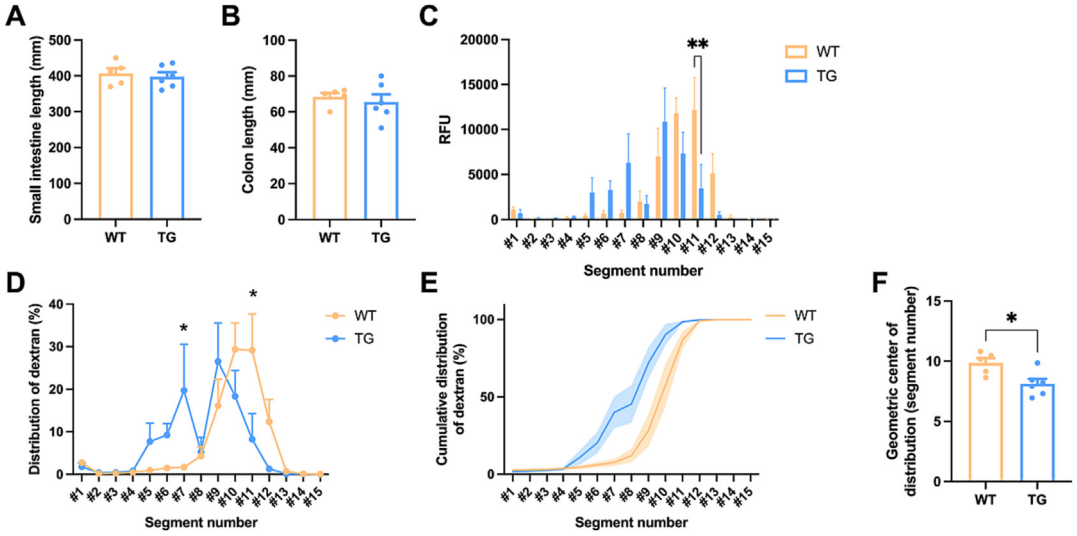

Fig. 1. Slower gastrointestinal transit in 5XFAD transgenic AD model mice than in WT. (A and B) The length of the small intestine and colon (mm) in WT (n = 6) and TG (n = 5) mice. **(C)** Relative fluorescence units (RFU) detected in 15 segments from the stomach to rectum. **(D)** Distribution of dextran (%), calculated by RFU of each segment normalized to total RFU. **(E)** Comparison of cumulative distributions of dextran of each genotype. **(F)** Comparison of the geometric center for distribution of dextran. Data are presented as mean ± SEM. * $P < 0.05$ and ** $P < 0.01$ by Student's *t*-test. WT, wild-type mice; TG, 5XFAD transgenic mice.

Worsened Aβ pathology in the TG-Lop group

We determined whether loperamide-induced slow gut transit could result in changes in amyloidopathy in the brain by quantifying the Aβ load using ELISA. Overall Aβ42 is composed of both soluble and insoluble Aβ42 (Fig. S7). There were no significant differences in the soluble Aβ42 levels between the TG-Con and TG-Lop groups in the cortex, hippocampus, and brain stem

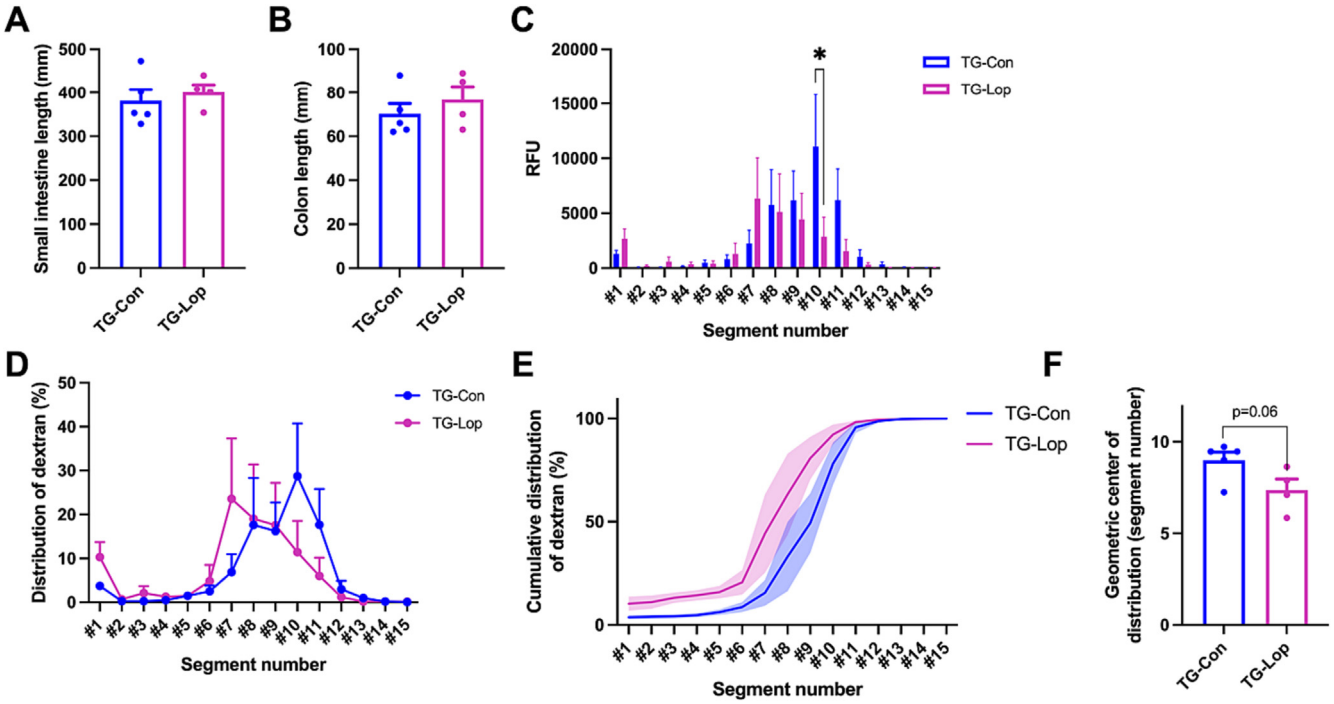

Fig. 2. Slowing of gastrointestinal transit by loperamide in 5XFAD transgenic AD mice. (A and B) The length of the small intestine and colon (mm) in TG-Con (n = 5) and TG-Lop (n = 4) mice. **(C)** Relative fluorescence units (RFU) detected in 15 segments from stomach to rectum. **(D)** Distribution of dextran (%), calculated by RFU of each segment normalized to total RFU. **(E)** Comparison of cumulative distributions of dextran of each group. **(F)** Comparison of the geometric center for distribution of dextran. Data are presented as mean ± SEM. *P < 0.05 by Student's t-test. Con, vehicle-treated control group; Lop, loperamide-treated group; TG, 5XFAD transgenic mice.

(Fig. 3A, D, and G, respectively). However, the loperamide-treated TG group demonstrated significantly increased insoluble and total Aβ42 levels in the cortex (Fig. 3B, C). We observed no significant differences in the Aβ levels between the TG-Con and TG-Lop groups in the hippocampus (Fig. 3D-F). However, the TG-Lop group had significantly higher insoluble and total Aβ levels in the brainstem compared to the TG-Con group (Fig. 3H, I). Our results suggest that the slow gut transit model of 5XFAD TG mice resulted in an increased Aβ load in the brain, especially in the cortex and brainstem.

Histological validation of Aβ plaques and microglia

To investigate the effects of the loperamide-induced slow gut transit on AD pathology, we measured the number of Aβ plaques and glial cells in the brain. Immunofluorescence staining with thioflavin S for Aβ plaques and Iba1 for microglia revealed that the TG-Lop group had a significant increase in the number of Aβ plaques and microglia in the primary motor cortex, primary sensory cortex, and nucleus tractus solitarius (NTS) compared to the TG-Con group (Fig. 4A, B). In contrast, loperamide did not alter the number of microglia in the cortex or the NTS of WT mice (Fig. 4C and Fig. S8). The number of Aβ plaques was significantly higher in the cortex and brainstem of the TG-Lop group than in the TG-Con group (Fig. 4C). Staining of the brain sections revealed that loperamide led to a significantly higher number of microglia ($Iba1^+$) in the cortex, hippocampus, and brain stem (Fig. 4D). However, we observed no differences in the number of astrocytes ($GFAP^+$) between the TG-Con and TG-Lop groups (Fig. 4C and Fig. S9).

Impaired visuospatial memory in slow gut model

We performed an OFT and NPR tests to assess locomotor activity and visuospatial memory, respectively. Neither loperamide nor the genotype affected locomotor activity (Fig. S10). In NPR tests, two objects were placed symmetrically at two points away from a visual cue (Location A and A') in the NPR test box. The mice were then placed in the center of the test box to explore the objects (*Acquisition phase*, Fig. 5A). After 24 h, one object was moved to a novel location (Location N), while the other remained in a familiar location (Location F), and the test trial was conducted for 10 min (*Test phase* in Fig. 5A). In the test phase, the WT-Lop group showed similar interaction times in both locations N and F, whereas the Con group spent more time in location N (32.09% vs. 67.91%, respectively; $p < 0.05$; Fig. 5B). The discrimination index revealed that the WT-Lop group had no values significantly different from zero, whereas the WT-Con group had a significantly different value from zero (Fig. 5C). Representative trajectories and two-dimensional (2D) heatmap plots revealed that the WT-Con group preferred the novel location over the familiar location, whereas the WT-Lop group presented an exploration pattern that was similarly distributed across both locations (Fig. 5D). Both TG-Con and TG-Lop groups showed similar interaction times at both locations (Fig. 5E). There were no significant differences in the discrimination index between the TG-Con and TG-Lop groups (Fig. 5F). Additionally, both TG-Con and TG-Lop groups presented an exploration pattern that was similarly distributed at both locations in the trajectories and 2D heatmap plots (Fig. 5G).

Transcriptome analysis of colon tissue

To investigate the effects of a slow gut transit and genotype, we performed RNA-seq on the colon tissues from the TG-Con, TG-Lop, WT-Con, and WT-Lop groups. In addition, we quantified the selected genes related to AD pathology and gut functions using qRT-PCR. The loperamide-treated group showed decreased mRNA levels of zonula occludens-1 (ZO-1), a tight junction protein, compared with the non-treated group (Fig. S11I).

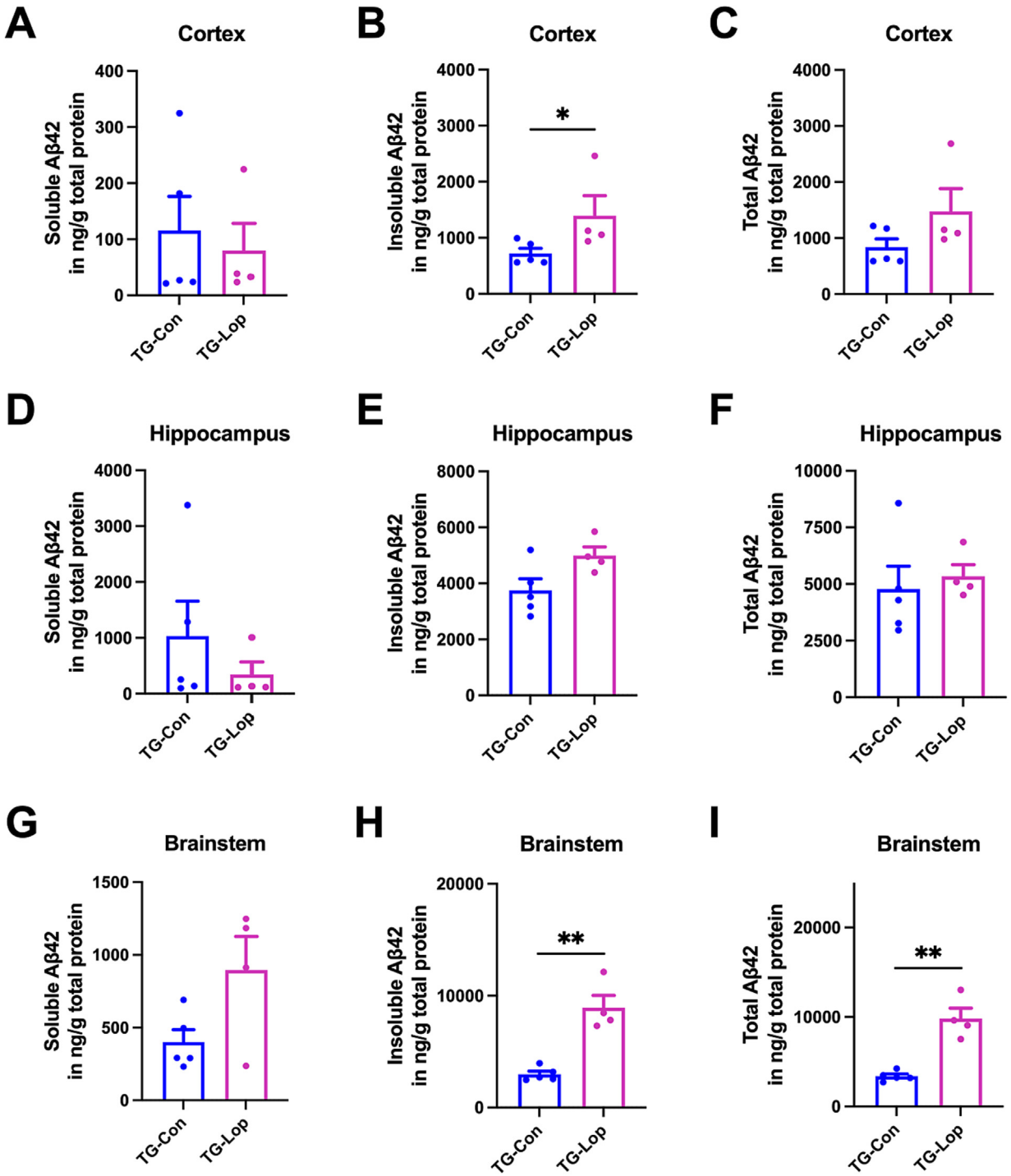

Fig. 3. Increased Aβ load by loperamide in 5XFAD transgenic AD mice. (A-C) ELISA quantification of Aβ42 in the cortex. **(A)** Soluble, **(B)** insoluble, and **(C)** total levels of Aβ42 in TG-Con (n = 5) and TG-Lop (n = 4) groups. **(D-F)** ELISA quantification of Aβ42 in the hippocampus. **(D)** Soluble, **(E)** insoluble, and **(F)** total levels of Aβ42 in TG-Con and TG-Lop groups. **G to I** ELISA quantification of Aβ42 in the cortex. **(G)** Soluble, **(H)** insoluble, and **(I)** total levels of Aβ42 in TG-Con and TG-Lop groups. Data are presented as mean ± SEM. * $P < 0.05$ and ** $P < 0.01$ by two-tailed Student's *t*-test and Mann-Whitney test. Con, vehicle-treated control group; ELISA, enzyme-linked immunosorbent assay; Lop, loperamide-treated group; TG, 5XFAD transgenic mice.

Principal components analysis (PCA) was performed to identify the major effectors of the colon transcriptome between the genotype and loperamide (Fig. 6A). Gut transcriptome is affected by both the genotype and loperamide. In a DEG analysis, 58 genes were upregulated, and 193 genes were downregulated in the TG-Con group compared with those in the WT-Con group (Fig. S12A). In the TG-Lop group, 39 differentially expressed genes (DEGs) were upregulated, and 100 genes were downregulated DEGs in comparison to the TG-Con group (Fig. S12B). After loperamide treatment in the WT group, 43 genes were upregulated, and 155 genes were downregulated compared with those in the WT-Con group (Fig. S12C).

RNA-seq analysis of the TG-Lop, TG-Con, and WT-Lop groups revealed 21 common DEGs that demonstrated more than a 2-fold increase compared to the WT-Con groups (Fig. 6B) and 66 DEGs with above a 2-fold decrease compared to the WT-Con group

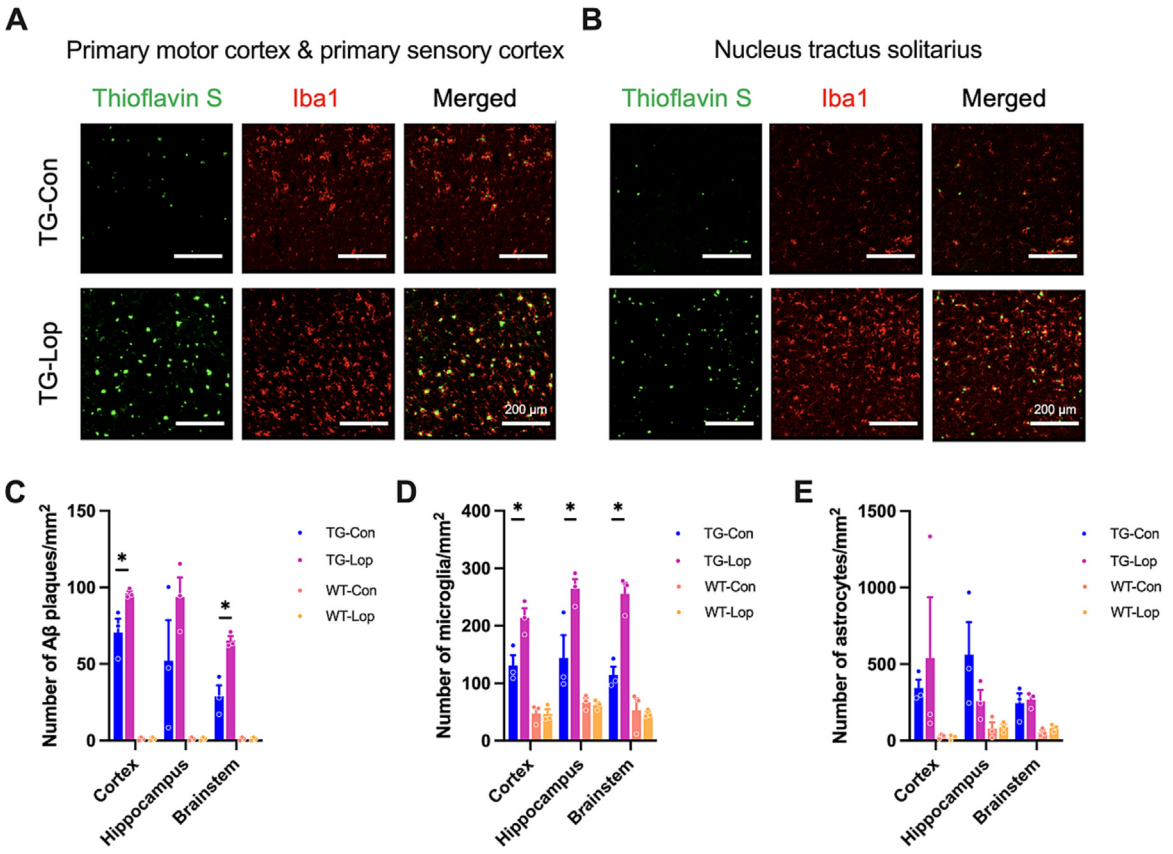

Fig. 4. Increased Aβ plaques and microglia by loperamide in 5XFAD transgenic AD mice. (A) Representative images of Aβ plaques (Thioflavin S; Green) and microglia (Iba1; Red) in the primary motor cortex and primary sensory cortex (Scale bar, 200 μm). **(B)** Representative images of Aβ plaques and microglia in the nucleus tractus solitarius (Scale bar, 200 μm). **(C)** Quantification of the number of Aβ plaques per unit area in the cortex, hippocampus, and brainstem. **(D)** Quantification of the number of microglia (Iba1 + cells) per unit area in the cortex, hippocampus, and brainstem. **(E)** Quantification of the number of astrocytes (GFAP + cells) per unit area in the cortex, hippocampus, and brainstem by unbiased stereology. Data are presented as mean ± SEM. * $P < 0.05$ by Student's *t*-test. Con, vehicle-treated control group; GFAP, glial fibrillary acidic protein; Iba1, ionized calcium-binding adaptor molecule 1; Lop, loperamide-treated group; TG, 5XFAD transgenic mice; WT, wild-type mice. (For interpretation of the references to colour in this figure legend, the reader is referred to the web version of this article.)

(Fig. 6C). KEGG enrichment analysis in the Enrichr database indicated that commonly upregulated DEGs between the three groups compared to the WT-Con groups were enriched in the mTOR signaling pathway (Fig. 6D). The 66 common down-regulated DEGs among the three groups were enriched in several pathways of the Elsevier pathway collection in the Enrichr database, including neurotropic factor deprivation in retinal ganglion cell death, ERK5/MAPK-7 signaling, apoptosis, mitochondrial fusion and fission, mitochondrial enlargement, and apoptosis in AD (Fig. 6D). In addition, the 15 downregulated DEGs among the TG-Con, TG-Lop, and WT-Con groups are indicated as gene lists with cutoff conditions of p < 0.05 and |log2(fold change)| >2 compared to WT-Con group (Fig. S13).

Enriched genes in norepinephrine secretion and immune response in TG

Gene set enrichment analysis (GSEA) was performed to determine the differentially enriched gene set between the TG-Con and WT-Con groups. The top 20 pathways based on the normalized enrichment score (NES) values in both groups were identified (Fig. 6E). Among the highly ranked pathways, the TG-Con group had enriched genes in pathways including norepinephrine secretion (NES = 1.435, nominal p-value or NOM-p < 0.001; Fig. 6F) and regulation of natural killer cell activation (NES = 1.354, NOM-p < 0.001; Fig. 6G). The loperamide-treated WT group also showed enriched genes involved in pathways, such as norepinephrine secretion, regulation of B cell proliferation, and synapse maturation (Fig. S14A, B). The WT-Con group showed increased gene sets suppressing interleukin-17 (IL-17) production (NES = – 1.435, NOM-p < 0.001; Fig. 6H) and B cell proliferation (NES = – 1.457, NOM-p < 0.001; Fig. 6I).

Reduced regulation of defense response to microbes in the TG-Lop group

To investigate the effects of slow gut transit in the AD mouse model, we performed GSEA between the TG-Lop and TG-Con groups (Fig. S15A). Stress granule assembly (NES = 1.460, NOM-p < 0.001; Fig. S15B) was ranked among the top 20 most relevant pathways between the TG-Lop and TG-Con groups. In addition, the GSEA plot revealed that the TG-Lop group had lower expression in the pathways that included mature B cell differentiation (NES = -1.481, NOM-p < 0.001; Fig. S15C) and regulation of defense response to the bacterium (NES = – 1.440, NOM-p < 0.001; Fig. S15D) than the TG-Con group.

No changes in mucosal microbiomes by genotype and gut transit

We performed taxonomic profiling of the mucosa-attached microbiome using a whole transcriptome analysis of the colon. To calculate the beta-diversity, we calculated the Bray-Curtis dissimilarity and unweighted and weighted UniFrac. Beta-diversity-based principal coordinate analysis (Fig. S15A) revealed no

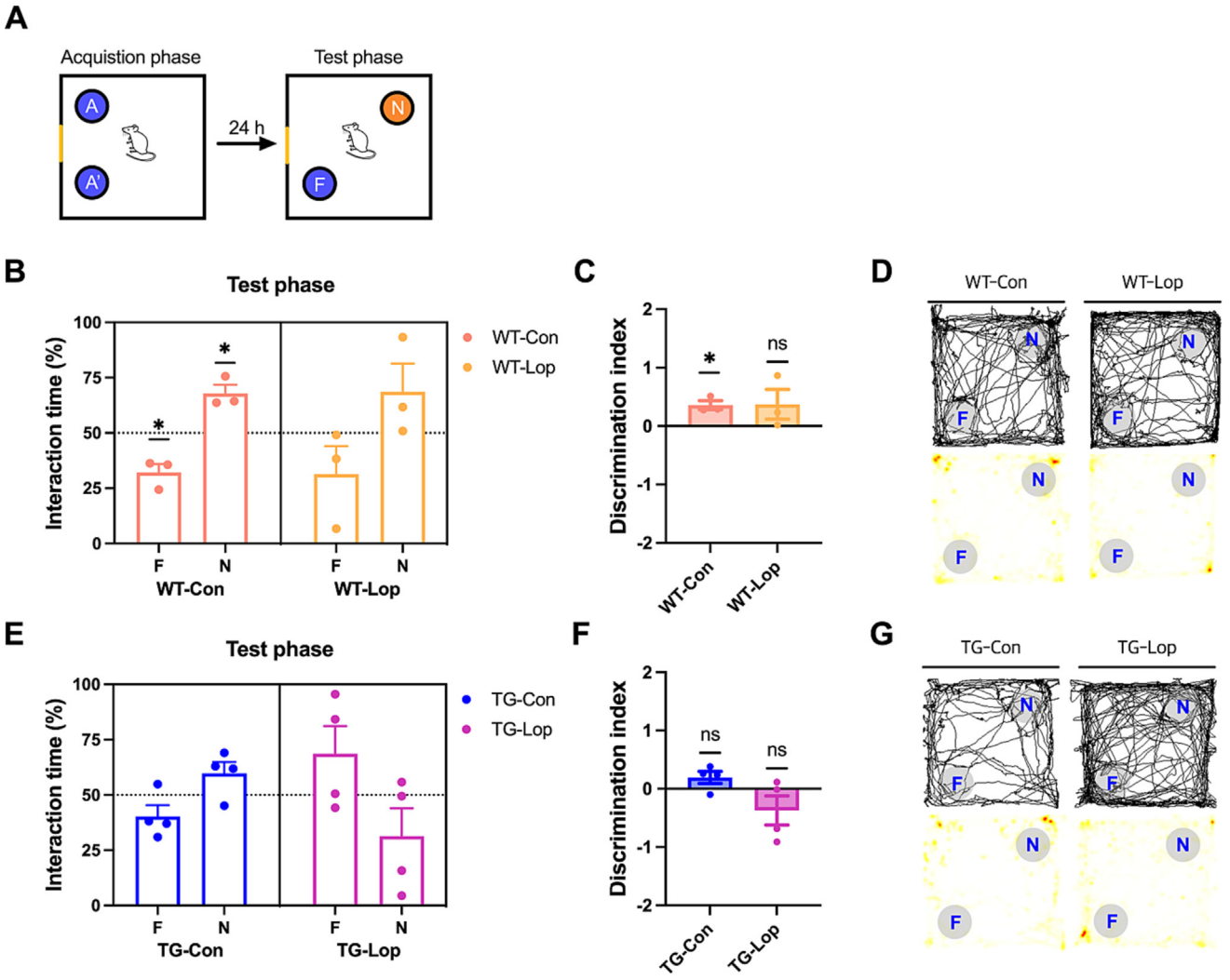

Fig. 5. Impaired visuospatial memory by loperamide in wild-type mice. (A) Schematic diagram of the novel place recognition (NPR) task. Circles with A and A' denote two identical objects at locations symmetrical to the visual cue (yellow line). Circles with F and N represent familiar and novel locations. See the method section for more detailed procedures. **(B)** The interaction time in a novel location (N) and familiar location (F) of the WT-Con (n = 3) and WT-Lop (n = 3) groups. **(C)** The discrimination index of the mice in the WT-Con and WT-Lop groups. **(D)** The representative trajectories and 2D heatmap plots of the WT-Con and WT-Lop mice in the test phase. Light grey circles indicate the location F and N in the test phase. **(E)** The interaction time in the novel and familiar locations of the TG-Con (n = 4) and TG-Lop (n = 4) mice. **(F)** The discrimination index of mice in the TG-Con and TG-Lop groups. **(G)** The representative trajectories and 2D heatmap plots of the TG-Con and TG-Lop mice in the test phase. The interaction times for each location are expressed as a percentage of the total exploration time and as the statistical difference against a 50 % theoretical mean. The discrimination index is tested against the '0' theoretical mean. Data are presented as mean ± SEM. * $P < 0.05$ by Student's *t*-test. Con, vehicle-treated control group; F, familial location; Lop, loperamide-treated group; N, novel location; ns, not statistically significant; TG, 5XFAD transgenic mice; WT, wild-type mice. (For interpretation of the references to colour in this figure legend, the reader is referred to the web version of this article.)

significantly different results among the four groups, including TG-Con, TG-Lop, WT-Con, and WT-Lop groups (Fig. S16B, C). Alpha diversity analyzed using the Shannon index also showed no difference among the four groups (Fig. S16D). At the phylum level, the relative abundance of *Proteobacteria* was lower in the TG-Con group than that in the WT group (Fig. S16E, F).

Discussion

We performed a comprehensive analysis of the relationship between slow gut transit and AD using bi-national epidemiological studies and mouse models. Epidemiological data from South Korea and Japan, involving more than 7.5 million participants, established a significant association between constipation and an increased risk of AD. In addition, we found a slower gastrointestinal transit in 5XFAD AD model mice than in WT mice. More interestingly, loperamide led to accelerated Aβ accumulation, increased microglia in the brain of the AD mice, and decreased transcription of tight junctions and memory, even in WT mice. Based on the transcriptomic analysis of the colon, AD mice showed the upregulation of norepinephrine secretion and immune response pathways more than the WT mice, and loperamide activated stress granule assembly and attenuated the defense response to microbes in TG mice. To the best of our knowledge, this is the first report to demonstrate a causal relationship between slow gut transit and AD pathology, thus indicating the potential of targeting gut motility as a novel therapeutic approach for AD.

Constipation has been regarded as a modifiable lifestyle factor or an aggravating factor in AD; however, only a few epidemiological studies have evaluated the link between constipation and AD [32]. Despite these associations, clinical studies have faced challenges in determining the direct effects of constipation on AD owing to the vagueness of its definition, high prevalence, various

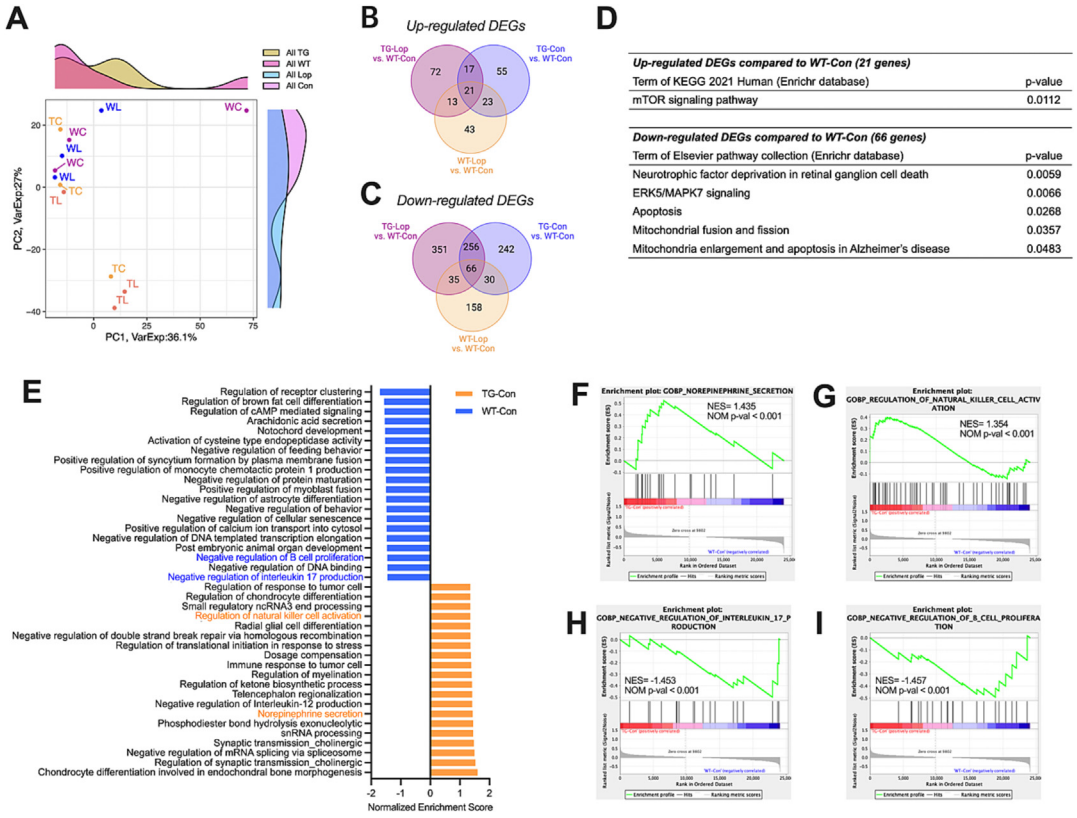

Fig. 6. Transcriptomic analysis of colon tissue. (**A**) Principal coordinate analysis plot of the four groups (n = 3 per each group), including TG-Con (TC), TG-Lop (TL), WT-Con (WC), and WT-Lop (WL). (**B**) Venn diagram showing the distribution of the upregulated DEGs of TG-Lop, TG-Con, and WT-Lop relative to WT-Con (p-value < 0.05 and Log2 (Fold change) > 1). (**C**) Venn diagram showing the distribution of the downregulated DEGs of TG-Lop, TG-Con, and WT-Lop relative to WT-Con (p-value < 0.05 and Log2(Fold change) < 1). (**D**) Functional classification of common DEGs (21 commonly up-regulated DEGs and 66 commonly down-regulated DEGs, respectively) by the Enrichr database. (**E**) The bar plot for GSEA results as the top twenty positively and negatively enriched pathways of the TG-Con group relative to the WT-Con group, respectively based on the NES (NOM p-value < 0.001). (**F-I**) Representative enrichment plots of GO_BP pathways from GSEA analysis between the TG-Con and WT-Con groups. (**F**) Norepinephrine secretion (NES = 1.435). (**G**) Regulation of natural killer cell activation (NES = 1.354). (**H**) Negative regulation of interleukin 17 production (NES = − 1.453). (**I**) Negative regulation of B cell proliferation (NES = − 1.457). Con, vehicle-treated control group; DEG, differentially expressed gene; GSEA, gene set enrichment analysis; GO_BP, gene ontology biological process; Lop, loperamide-treated group; NES, normalized enrichment score; NOM p-value, nominal p-value; TG, 5XFAD transgenic mice; VarExp, explained variance; WT, wild-type mice.

causes, and high comorbidities in the elderly [33]. However, our findings suggest a significant association between AD and constipation based on large cohorts from two countries, which included a total of 7,509,478 participants.

5XFAD AD mice exhibited slower gastrointestinal transit than WT mice, possibly due to enteric nervous system (ENS) dysfunction. TG mice also displayed higher norepinephrine secretion and immune response pathways, thus suggesting a mechanistic link between slow gut transit and AD progression. In AD mice, reduced neural density in the myenteric networks, which is an indicator of ENS impairment, has preceded the accumulation of Aβ in the brain [34]. In addition, the loss of nitrergic and cholinergic neurons in the ileum of AD model mice has been associated with increased inflammation and the number of macrophages in the intestine, thus suggesting a connection between ENS impairment and intestinal inflammation in AD [35]. Regarding the specific findings of the study, it was observed that TG mice showed slower gut transit compared to WT mice, potentially due to ENS dysfunction. The TG group also had increased gene sets involved in the norepinephrine secretion in the colon compared to the WT group. Norepinephrine, a neurotransmitter from the sympathetic nerves in the gut, regulates gut contractions, leading to the reduction in gut motility [36]. The possibility of gut transit slowing down due to ENS impairment or brainstem amyloidopathy in vagal efferents has been investigated as a contributing factor to AD [37].

Slow intestinal motility may result in the deterioration of intestinal health [38]. Subsequent bacterial overgrowth in the gut may lead to an imbalance in the gut microbiota, which is known to play a role in brain health [39]. Bacterial overgrowth can also disrupt the intestinal barrier, thus allowing harmful substances, such as bacterial toxins and byproducts, to enter the bloodstream [40]. The WT group showed suppressed IL-17 secretion pathways in the colon compared to the TG group. IL-17 is a cytokine secreted by Th17 cells and is a marker of increased gastrointestinal inflammation, which is observed in patients with colorectal cancer or inflammatory bowel diseases [41]. Increased gastrointestinal inflammation in the TG group can contribute to systemic inflammation through the gut-brain axis [42], thus resulting in neuroinflammation and induction of a leaky gut through the gut-brain axis [43]. Our results also revealed that the TG-Con group had activated regulation of natural killer cell activation and suppressed gene sets involved in the negative regulation of B cell proliferation compared to the WT group. The interplay between the gut and the brain forms a vicious cycle that accelerates disease progression. Therefore, understanding the gut-brain axis and its role in neurodegenerative diseases is essential for identifying potential therapeutic targets [44]. Treatments targeting the ENS or vagus nerve could potentially alleviate some of the symptoms or even slow the progression of AD [45].

To understand whether slow gut transit accelerates the disease process in AD, we used loperamide as an experimental agent for

slowing gut transit. Loperamide, a drug that cannot cross the blood–brain barrier [46], is a widely used over-the-counter antidiarrheal medication that acts on the μ-opioid receptors in the ENS to slow down gut motility. Its mechanism involves the inhibition of calcium channels in the neuromuscular junctions, thus leading to decreased neurotransmitter release, such as acetylcholine, and subsequent relaxation of the smooth muscles in the gut [47]. Mice treated with loperamide showed slower gut transit time than the control mice.

Consistent with our hypothesis that slowing gut transit would accelerate AD pathology, Aβ load in the brain was increased in the loperamide-treated AD mouse model. In association with robust amyloidopathy, the TG-Lop group showed an increased number of microglia in the brain. Notably, changes in the intestine caused by loperamide accelerated the worsening of AD pathology in the brain. Previous studies have suggested that the loperamide-induced constipation model revealed alterations in the microbiome compositions and gut dysbiosis [48]. Furthermore, slow gut transit is associated with increased gut dysbiosis and permeability, which can result in a leaky gut [49]. Lower mRNA levels of ZO-1, a tight junction protein, in the loperamide-treated groups also suggest an impairment of the gut barrier function and increased intestinal permeability, thus resulting in the translocation of bacteria and toxins into the bloodstream [50].

Compared with the TG-Con group, the TG-Lop group showed decreased transcription of genes that regulate the defense responses to the bacteria. In addition, stress granule assembly and cellular responses to various stressors, such as viral infection [51], were activated in the TG-Lop group. Given that constipation increases intestinal reactive oxygen species and cellular stress [52], it is plausible that loperamide-induced constipation imposes a similar stress on the intestinal tissues, which was evident in our data. Furthermore, our colonic transcriptome data are consistent with the leaky gut states. AD has been linked with the gut-brain axis and dysbiosis in clinical studies [53]. As a damaged gut barrier with lipopolysaccharides resulted in microglial activation, neuroinflammation, and cognitive decline [54], we postulated that the slow gut transit induces gut dysbiosis and overgrowth of bacteria, which, in turn, disrupts the intestinal barrier and triggers systemic inflammation and neuroinflammation. We believe the change in intestinal tissue into a leaky gut might have been the initial step in accelerating the pathogenesis of AD via the gut-brain axis.

We believe that the gut-brain axis plays a role in this process. Constipation can influence the gut microbiome, and conversely, microbiome dysbiosis can cause constipation [55]. Nevertheless, several studies have reported that the composition of the gut microbiome in patients with AD is altered [56,57], and that this altered microbiome can provoke an inflammatory response systemically and transfer intestinal toxic metabolites to the brain using the vagus nerve as a conduit [45]. In addition, an altered gut microbiome can affect neuroinflammation and neuronal activity by secreting cytokines and metabolites that interact with intestinal mucosal cells [58,59]. Neuroinflammation causes cognitive impairment [60,61]; therefore, changes in the gut-brain axis could lead to memory impairment in groups treated with loperamide [62]. We examined the gut microbiome using whole RNA-sequencing of colon tissue, which represents the mucosal microbiome. However, we did not find any significant alterations in the mucosal microbiome from our colon samples. Our findings cannot exclude the possibility of gut dysbiosis because the mucosal microbiome is distinct from the luminal microbiome and is more stable under environmental challenges, such as abnormalities in gut motility [63].

We found more retroperitoneal adipose tissue surrounding the gastrointestinal tract in the TG group compared to the WT group, which is consistent with previous studies that suggested a potential link between adipose tissue distribution and AD [64]. Adipose tissue, particularly retroperitoneal adipose tissue, can have systemic effects, including modulation of inflammatory processes and metabolic functions [64]. In addition, retroperitoneal adipose tissue influences the gut, and its microbiome is significantly associated with the pathological process of AD [65].

Our findings suggested a causal relationship between slow gut and AD using binational epidemiological data and AD mouse models. Using discovery and validation cohorts, we suggested that constipation was significantly associated with the risk of AD; furthermore, the AD mouse model showed a significant slowing of gut transit compared to their wild-type counterparts. Loperamide worsened the deposition of Aβ plaques and microglial responses in the brain, thus suggesting that a slow gut transit may be a critical contributor to the pathogenesis of AD. Based on the results of this study, we propose that gut transit or motility may be a disease-modifying lifestyle factor in AD.

Strengths and limitations

This binational, population-based, large-scale cohort study benefited from a large diverse sample size. This approach minimizes selection bias and improves the potential for generalization. We provided epidemiological evidence from human cohorts and insights into the underlying mechanisms through animal experimental studies to explore the association between constipation and AD (Table S5). In addition, we pioneered the use of a loperamide-induced constipation model in AD mice (Table S1). Furthermore, we aimed to observe the effects of slow gut transit on AD pathology from various perspectives, including transcriptomic, metagenomic, molecular, and behavioral analyses.

However, our study has several limitations. First, this dataset was not generated for research purposes but rather for insurance claims. Therefore, the information provided included only enrolled individuals, which introduces a potential selection bias. However, in South Korea, where the entire population is covered by insurance, the dataset utilized can be considered representative of the entire population [66], thus mitigating the risk of selection bias. In contrast, the JMDC data do not cover claims information for the entire population, which results in a relatively higher risk of selection bias [67]. To address this limitation, we conducted a binational cohort study and performed analyses stratified by age and sex. In addition, we conducted analyses based on the duration of constipation morbidity to enhance the robustness of the findings. Second, this retrospective cohort study lacked a complete control for confounding variables, including the dietary habits of the participants, which could have been collected through surveys or personal investigations (Table S6). To address this issue, we attempted to control for confounding variables using propensity score matching. Additionally, we derived more robust results by calculating the adjusted hazard ratios. Third, we defined the diseases using ICD-10 codes. However, previous validation studies showed high positive predictive values between 0.80 and 0.91, and this method is commonly used in previous studies [67–72]. Fourth, we observed that the slow gut transit model in TG mice resulted in significant increases in Aβ load in the cortex and brainstem. Therefore, further experiments focusing on the functional and behavioral parameters associated with these regions are warranted. Such an investigation could provide valuable insights into the broader understanding of Alzheimer's disease pathology. Fifth, the scope of our study was primarily limited to transcriptomic changes, Aβ load, alterations in glial cells, and working memory functions relevant to AD pathology. The study could have benefited from the inclusion of an evaluation of reactive oxygen species levels, tau pathology,

proinflammatory cytokines levels, and markers of apoptosis, autophagy, and mitochondrial dysfunction. However, owing to methodological constraints, our study did not include these aspects. Further studies are needed to explore these aspects and provide a more comprehensive view of the pathophysiology of the disease.

Compliance with ethics requirements

All animal procedures were approved by the ethics committee at the Gwangju Institute of Science and Technology (GIST -2020-031) following the Institutional Animal Care and Use Committee guidelines. This study was approved by the Institutional Review Boards of the Kyung Hee University (KHUH 2022-06-042). The requirement for informed consent was waived because this study used de-identified administrative data. Data availability: Data are available on reasonable request. Study protocol, statistical code: available from DKY (email: yonkkang@gmail.com). Data set: available from the National Health Insurance Service (NHIS) of South Korea through a data use agreement. Code availability: All statistical codes required to reanalyze the data are available upon request.

Declaration of Competing Interest

The authors declare that they have no known competing financial interests or personal relationships that could have appeared to influence the work reported in this paper.

Acknowledgements

The work was supported by grants from the Ministry of Health&Welfare (HI22C046700 and HU22C0150), the Ministry of Science&ICT (NRF-2022R1A2C3009749 and RS-2023-00248157), the Ministry of Culture, Sports, and Tourism (R2022020030), and the GIST Research Institute (GRI) IIBR grant funded by the GIST in 2023. Graphical abstract is created with Biorender (https://biorender.com/) and exported under a paid subscription.

Appendix A. Supplementary data

Supplementary data to this article can be found online at https://doi.org/10.1016/j.jare.2023.12.010.

References

[1] Shin A. The changing prevalence of functional constipation: why words matter. Lancet Gastroenterol Hepatol 2021;6(8):600–2.
[2] Barberio B, Judge C, Savarino EV, Ford AC. Global prevalence of functional constipation according to the Rome criteria: a systematic review and meta-analysis. Lancet Gastroenterol Hepatol 2021;6(8):638–48.
[3] Drossman DA, Hasler WL. Rome IV-Functional GI Disorders: Disorders of Gut-Brain Interaction. Gastroenterology 2016;150(6):1257–61.
[4] Chu H, Zhong L, Li H, Zhang X, Zhang J, Hou X. Epidemiology characteristics of constipation for general population, pediatric population, and elderly population in china. Gastroenterol Res Pract 2014;2014(532734.
[5] Savica R, Boeve BF, Mielke MM. When Do alpha-Synucleinopathies Start? An Epidemiological Timeline: A Review. JAMA Neurol 2018;75(4):503–9.
[6] Camacho M, Macleod AD, Maple-Grodem J, Evans JR, Breen DP, Cummins G, et al. Early constipation predicts faster dementia onset in Parkinson's disease. NPJ Parkinsons Dis 2021;7(1):45.
[7] Zakrzewska-Pniewska B, Gawel M, Szmidt-Salkowska E, Kepczynska K, Nojszewska M. Clinical and functional assessment of dysautonomia and its correlation in Alzheimer's disease. Am J Alzheimers Dis Other Demen 2012;27(8):592–9.
[8] Yang Z, Wei C, Li X, Yuan J, Gao X, Li B, et al. Association Between Regular Laxative Use and Incident Dementia in UK Biobank Participants. Neurology 2023;100(16):e1702–11.
[9] Vazquez Roque M, Bouras E P. Epidemiology and management of chronic constipation in elderly patients. Clin Interv Aging 2015;10(919-930.
[10] Nightingale JMD, Paine P, McLaughlin J, Emmanuel A, Martin JE, Lal S, et al. The management of adult patients with severe chronic small intestinal dysmotility. Gut 2020;69(12):2074–92.
[11] Baidoo N, Sanger GJ, Belai A. Effect of old age on the subpopulations of enteric glial cells in human descending colon. Glia 2023;71(2):305–16.
[12] Broad J, Kung VWS, Palmer A, Elahi S, Karami A, Darreh-Shori T, et al. Changes in neuromuscular structure and functions of human colon during ageing are region-dependent. Gut 2019;68(7):1210–23.
[13] Liu L, Milkova N, Nirmalathasan S, Ali MK, Sharma K, Huizinga JD, et al. Diagnosis of colonic dysmotility associated with autonomic dysfunction in patients with chronic refractory constipation. Sci Rep 2022;12(1):12051.
[14] Jost WH. Gastrointestinal motility problems in patients with Parkinson's disease. Effects of antiparkinsonian treatment and guidelines for management. Drugs Aging 1997;10(4):249–58.
[15] Zhang T, Han Y, Wang J, Hou D, Deng H, Deng Y L, Song Z. Comparative Epidemiological Investigation of Alzheimer's Disease and Colorectal Cancer: The Possible Role of Gastrointestinal Conditions in the Pathogenesis of AD. Front Aging Neurosci 2018;10(176.
[16] Alam MZ, Alam Q, Kamal MA, Abuzenadah AM, Haque A. A possible link of gut microbiota alteration in type 2 diabetes and Alzheimer's disease pathogenicity: an update. CNS Neurol Disord Drug Targets 2014;13(3):383–90.
[17] Naseer MI, Bibi F, Alqahtani MH, Chaudhary AG, Azhar EI, Kamal MA, et al. Role of gut microbiota in obesity, type 2 diabetes and Alzheimer's disease. CNS Neurol Disord Drug Targets 2014;13(2):305–11.
[18] Attaluri A, Jackson M, Valestin J, Rao SS. Methanogenic flora is associated with altered colonic transit but not stool characteristics in constipation without IBS. Am J Gastroenterol 2010;105(6):1407–11.
[19] Carabotti M, Scirocco A, Maselli MA, Severi C. The gut-brain axis: interactions between enteric microbiota, central and enteric nervous systems. Ann Gastroenterol 2015;28(2):203–9.
[20] Borre YE, O'Keeffe GW, Clarke G, Stanton C, Dinan TG, Cryan JF. Microbiota and neurodevelopmental windows: implications for brain disorders. Trends Mol Med 2014;20(9):509–18.
[21] Tian H, Chen Q, Yang B, Qin H, Li N. Analysis of Gut Microbiome and Metabolite Characteristics in Patients with Slow Transit Constipation. Dig Dis Sci 2021;66(9):3026–35.
[22] Mitrea L, Nemes S A, Szabo K, Teleky B E, Vodnar D C. Guts Imbalance Imbalances the Brain: A Review of Gut Microbiota Association With Neurological and Psychiatric Disorders. Front Med (Lausanne) 2022;9(813204.
[23] Suganya K, Gut-Brain KBS, Axis. Role of Gut Microbiota on Neurological Disorders and How Probiotics/Prebiotics Beneficially Modulate Microbial and Immune Pathways to Improve Brain Functions. Int J Mol Sci 2020;21(20).
[24] Seo DO, O'Donnell D, Jain N, Ulrich JD, Herz J, Li Y, et al. ApoE isoform- and microbiota-dependent progression of neurodegeneration in a mouse model of tauopathy. Science 2023;379(6628):eadd1236..
[25] Kim N, Jeon S H, Ju I G, Gee M S, Do J, Oh M S, Lee J K. Transplantation of gut microbiota derived from Alzheimer's disease mouse model impairs memory function and neurogenesis in C57BL/6 mice. Brain Behav Immun 2021;98(357-365.
[26] Pan RY, Zhang J, Wang J, Wang Y, Li Z, Liao Y, et al. Intermittent fasting protects against Alzheimer's disease in mice by altering metabolism through remodeling of the gut microbiota. Nat Aging 2022;2(11):1024–39.
[27] Cammann D, Lu Y, Cummings MJ, Zhang ML, Cue JM, Do J, et al. Genetic correlations between Alzheimer's disease and gut microbiome genera. Sci Rep 2023;13(1):5258.
[28] Ferreiro AL, Choi J, Ryou J, Newcomer EP, Thompson R, Bollinger RM, et al. Gut microbiome composition may be an indicator of preclinical Alzheimer's disease. Sci Transl Med 2023;15(700):eabo2984..
[29] Kim JE, Park JJ, Lee MR, Choi JY, Song BR, Park JW, et al. Constipation in Tg2576 mice model for Alzheimer's disease associated with dysregulation of mechanism involving the mAChR signaling pathway and ER stress response. PLoS One 2019;14(4):e0215205.
[30] Oakley H, Cole SL, Logan S, Maus E, Shao P, Craft J, et al. Intraneuronal beta-amyloid aggregates, neurodegeneration, and neuron loss in transgenic mice with five familial Alzheimer's disease mutations: potential factors in amyloid plaque formation. J Neurosci 2006;26(40):10129–40.
[31] Kang J, Park M, Lee E, Jung J, Kim T. The Role of Vitamin D in Alzheimer's Disease: A Transcriptional Regulator of Amyloidopathy and Gliopathy. Biomedicines 2022;10(8).
[32] Nakase T, Tatewaki Y, Thyreau B, Mutoh T, Tomita N, Yamamoto S, et al. Impact of constipation on progression of Alzheimer's disease: A retrospective study. CNS Neurosci Ther 2022;28(12):1964–73.
[33] Wagenaar MC, van der Putten AAJ, Douma JG, van der Schans CP, Waninge A. Definitions, signs, and symptoms of constipation in people with severe or profound intellectual disabilities: A systematic review. Heliyon 2022;8(5):e09479.
[34] Semar S, Klotz M, Letiembre M, Van Ginneken C, Braun A, Jost V, et al. Changes of the enteric nervous system in amyloid-beta protein precursor transgenic mice correlate with disease progression. J Alzheimers Dis 2013;36(1):7–20.
[35] Han X, Tang S, Dong L, Song L, Dong Y, Wang Y, Du Y. Loss of nitrergic and cholinergic neurons in the enteric nervous system of APP/PS1 transgenic mouse model. Neurosci Lett 2017;642(59-65.
[36] Kurahashi M, Kito Y, Hara M, Takeyama H, Sanders KM, Hashitani H. Norepinephrine Has Dual Effects on Human Colonic Contractions Through Distinct Subtypes of Alpha 1 Adrenoceptors. Cell Mol. Gastroenterol Hepatol 2020;10(3):658–671 e651.
[37] Fulling C, Dinan TG, Cryan JF. Gut Microbe to Brain Signaling: What Happens in Vagus. Neuron 2019;101(6):998–1002.

[38] Bitar K, Greenwood-Van Meerveld B, Saad R, Wiley JW. Aging and gastrointestinal neuromuscular function: insights from within and outside the gut. Neurogastroenterol Motil 2011;23(6):490–501.
[39] Sharon G, Sampson TR, Geschwind DH, Mazmanian SK. The Central Nervous System and the Gut Microbiome. Cell 2016;167(4):915–32.
[40] Wang Y, Kasper L H. The role of microbiome in central nervous system disorders. Brain Behav Immun 2014;38(1-12.
[41] De Simone V, Franze E, Ronchetti G, Colantoni A, Fantini MC, Di Fusco D, et al. Th17-type cytokines, IL-6 and TNF-alpha synergistically activate STAT3 and NF-kB to promote colorectal cancer cell growth. Oncogene 2015;34 (27):3493–503.
[42] Dodiya HB, Kuntz T, Shaik SM, Baufeld C, Leibowitz J, Zhang X, et al. Sex-specific effects of microbiome perturbations on cerebral Abeta amyloidosis and microglia phenotypes. J Exp Med 2019;216(7):1542–60.
[43] Mou Y, Du Y, Zhou L, Yue J, Hu X, Liu Y, et al. Gut Microbiota Interact With the Brain Through Systemic Chronic Inflammation: Implications on Neuroinflammation, Neurodegeneration, and Aging. Front Immunol 2022;13 (796288.
[44] Sampson TR, Debelius JW, Thron T, Janssen S, Shastri GG, Ilhan ZE, et al. Gut Microbiota Regulate Motor Deficits and Neuroinflammation in a Model of Parkinson's Disease. Cell 2016;167(6):1469–1480 e1412.
[45] Bonaz B, Bazin T, Pellissier S. The Vagus Nerve at the Interface of the Microbiota-Gut-Brain Axis. Front Neurosci 2018;12(49.
[46] Baker D E. Loperamide: a pharmacological review. Rev Gastroenterol Disord 2007;7 Suppl 3(S11-18.
[47] Regnard C, Twycross R, Mihalyo M, Wilcock A. Loperamide. J Pain Symptom Manage 2011;42(2):319–23.
[48] Zhang X, Zheng J, Jiang N, Sun G, Bao X, Kong M, et al. Modulation of gut microbiota and intestinal metabolites by lactulose improves loperamide-induced constipation in mice. Eur J Pharm Sci 2021;158(105676.
[49] Camilleri M. Leaky gut: mechanisms, measurement and clinical implications in humans. Gut 2019;68(8):1516–26.
[50] Bischoff S C, Barbara G, Buurman W, Ockhuizen T, Schulzke J D, Serino M, et al. Intestinal permeability–a new target for disease prevention and therapy. BMC Gastroenterol 2014;14(189.
[51] Hofmann S, Kedersha N, Anderson P, Ivanov P. Molecular mechanisms of stress granule assembly and disassembly. Biochim Biophys Acta Mol Cell Res 2021;1868(1):118876.
[52] Vermorken AJ, Andres E, Cui Y. Bowel movement frequency, oxidative stress and disease prevention. Mol Clin Oncol 2016;5(4):339–42.
[53] Stadlbauer V, Engertsberger L, Komarova I, Feldbacher N, Leber B, Pichler G, et al. Dysbiosis, gut barrier dysfunction and inflammation in dementia: a pilot study. BMC Geriatr 2020;20(1):248.
[54] Kar F, Hacioglu C, Kar E, Donmez DB, Kanbak G. Probiotics ameliorates LPS induced neuroinflammation injury on Abeta 1–42, APP, gamma-beta secretase and BDNF levels in maternal gut microbiota and fetal neurodevelopment processes. Metab Brain Dis 2022;37(5):1387–99.
[55] Fu P, Gao M, Yung KKL. Association of Intestinal Disorders with Parkinson's Disease and Alzheimer's Disease: A Systematic Review and Meta-Analysis. ACS Chem Neurosci 2020;11(3):395–405.
[56] Vogt NM, Kerby RL, Dill-McFarland KA, Harding SJ, Merluzzi AP, Johnson SC, et al. Gut microbiome alterations in Alzheimer's disease. Sci Rep 2017;7 (1):13537.
[57] Jiang C, Li G, Huang P, Liu Z, Zhao B. The Gut Microbiota and Alzheimer's Disease. J Alzheimers Dis 2017;58(1):1–15.
[58] Veiga-Fernandes H, Mucida D. Neuro-Immune Interactions at Barrier Surfaces. Cell 2016;165(4):801–11.
[59] Chen C, Liao J, Xia Y, Liu X, Jones R, Haran J, et al. Gut microbiota regulate Alzheimer's disease pathologies and cognitive disorders via PUFA-associated neuroinflammation. Gut 2022;71(11):2233–52.
[60] Tian Z, Ji X, Liu J. Neuroinflammation in Vascular Cognitive Impairment and Dementia: Current Evidence, Advances, and Prospects. Int J Mol Sci 2022;23 (11).
[61] Zhao J, Bi W, Xiao S, Lan X, Cheng X, Zhang J, et al. Neuroinflammation induced by lipopolysaccharide causes cognitive impairment in mice. Sci Rep 2019;9 (1):5790.
[62] Yang X, Yu D, Xue L, Li H, Du J. Probiotics modulate the microbiota-gut-brain axis and improve memory deficits in aged SAMP8 mice. Acta Pharm Sin B 2020;10(3):475–87.
[63] Wu M, Li P, Li J, An Y, Wang M, Zhong G. The Differences between Luminal Microbiota and Mucosal Microbiota in Mice. J Microbiol Biotechnol 2020;30 (2):287–95.
[64] Huang X, Wang Y J, Xiang Y. Bidirectional communication between brain and visceral white adipose tissue: Its potential impact on Alzheimer's disease. EBioMedicine 2022;84(104263.
[65] Wang C, Yi Z, Jiao Y, Shen Z, Yang F, Zhu S. Gut Microbiota and Adipose Tissue Microenvironment Interactions in Obesity. Metabolites 2023;13(7).
[66] Shin YH, Shin JI, Moon SY, Jin HY, Kim SY, Yang JM, et al. Autoimmune inflammatory rheumatic diseases and COVID-19 outcomes in South Korea: a nationwide cohort study. Lancet Rheumatol 2021;3(10):e698–706.
[67] Nagai K, Tanaka T, Kodaira N, Kimura S, Takahashi Y, Nakayama T. Data resource profile: JMDC claims databases sourced from Medical Institutions. J Gen Fam Med 2020;21(6):211–8.
[68] Sommerlad A, Perera G, Singh-Manoux A, Lewis G, Stewart R, Livingston G. Accuracy of general hospital dementia diagnoses in England: Sensitivity, specificity, and predictors of diagnostic accuracy 2008–2016. Alzheimers Dement 2018;14(7):933–43.
[69] Tari AR, Nauman J, Zisko N, Skjellegrind HK, Bosnes I, Bergh S, et al. Temporal changes in cardiorespiratory fitness and risk of dementia incidence and mortality: a population-based prospective cohort study. Lancet Public Health 2019;4(11):e565–74.
[70] Brown A, Kirichek O, Balkwill A, Reeves G, Beral V, Sudlow C, et al. Comparison of dementia recorded in routinely collected hospital admission data in England with dementia recorded in primary care. Emerg Themes Epidemiol 2016;13 (11.
[71] Fujiyoshi A, Jacobs DR, Jr., Alonso A, Luchsinger J A, Rapp S R, Duprez D A. Validity of Death Certificate and Hospital Discharge ICD Codes for Dementia Diagnosis: The Multi-Ethnic Study of Atherosclerosis. Alzheimer Dis Assoc Disord 2017;31(2):168–72.
[72] Nedelec T, Couvy-Duchesne B, Monnet F, Daly T, Ansart M, Gantzer L, et al. Identifying health conditions associated with Alzheimer's disease up to 15 years before diagnosis: an agnostic study of French and British health records. Lancet Digit Health 2022;4(3):e169–78.